Inorg. Chem. **2006**, *45*, 6387–6395

Transition from a Nonbonding to a Bonding Interaction in a Tetranuclear $[Mo_2]_2(\mu\text{-OR})_4$ Cluster

F. Albert Cotton,* Zhong Li, Chun Y. Liu, Carlos A. Murillo,* and Qinliang Zhao

Department of Chemistry, Laboratory for Molecular Structure and Bonding, P.O. Box 30012, Texas A&M University, College Station, Texas 77842-3012

Received April 10, 2006

Tetranuclear Mo_4 clusters with two quadruply bonded Mo_2^{4+} units, $[Mo_2(cis\text{-DAniF})_2]$ (DAniF = *N*,*N*′-di-*p*-anisylformamidinate), linked by alkoxides (OCH_3 for **1** and OC_2H_5 for **4**) have been prepared. The nonbonding separation between the midpoints of the quadruply bonded units, ca. 3.24 Å, is the shortest among compounds having two linked Mo_2^{4+} units. Electrochemical measurements show two redox waves for each compound with large $\Delta E_{1/2}$ values (554 and 587 mV for **1** and **4**, respectively) that correspond to K_C values on the order of 10^9. The large electronic communication is attributed to the short separation between dinuclear units that favor direct δ-to-δ orbital interactions between the two dimetal centers. Compound **1** was chemically oxidized using stoichiometric amounts of ferrocenium salts to a one-electron oxidation product **2** (in which the counteranion is PF_6^-) and a two-electron oxidation product **3** (which contains two BF_4^- anions). Upon oxidation there are significant decreases in the distance between the two $[Mo_2]$ units to 3.100 Å and then to 2.945 Å. The mixed-valence species **2** shows two broad absorption bands at 5900 and 7900 cm^{-1} in the NIR region which are assigned to the HOMO-1 → SOMO and HOMO-2 → SOMO transitions. Compound **3** is fluxional in solution, as shown by variable-temperature ^1H NMR spectra. The sharp signals in the NMR spectrum at –50 °C and the lack of an EPR signal suggest that this species is diamagnetic and that a four-center, two-electron bond is formed in the cyclometallic Mo_4 cluster. To a first-order approximation, an average bond order of 0.25 is assigned to the bonding interaction between the two Mo atoms along the long edges of the rectangle defined by the four Mo atoms.

Introduction

Numerous cyclic tetranuclear compounds consisting of two triply or quadruply bonded dimetal units joined by four single-atom bridging ligands have been reported.[1,2] Such molybdenum compounds are sometimes collectively called rectangular Mo_4 clusters. Three important types (**I**, **II**, and **III)** are shown in Scheme 1. The bridging groups, X, used in such molecules have been of considerable variety. In compounds of type **I**, two quadruple bonds have undergone [2 + 2] cycloaddition to form a metallocyclobutadiyne ring by cleaving the δ bonds and then forming two σ bonds between the two dimolybdenum pairs, as shown in Scheme 2.[3] For example, in the tetrachloro-bridged compound

Scheme 1

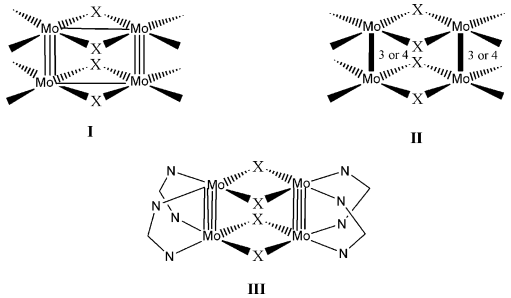

Scheme 2

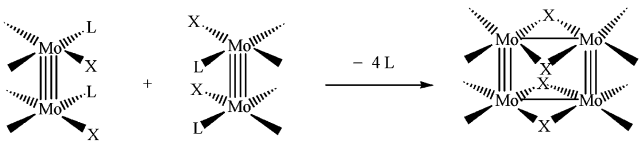

$Mo_4Cl_4(PEt_3)_4$, the short (ca. 2.21 Å) and long edges (2.90 Å) of the Mo_4 rectangle correspond to Mo≡Mo triple bonds

* To whom correspondence should be addressed. E-mail: cotton@tamu.edu (F.A.C.); murillo@tamu.edu (C.A.M.).

(1) Chisholm, M. H.; Macintosh, A. M. *Chem. Rev.* **2005**, *105*, 2929.
(2) See for example: (a) Carlin, R. T.; McCarley, R. E. *Inorg. Chem.* **1989**, *28*, 3432. (b) Schrock, R. R.; Sturgeoff, L. G.; Sharp, P. R. *Inorg. Chem.* **1983**, *22*, 2801. (c) Bera, J. K.; Lau, S. S.; Fanwick, P. E.; Walton, R. A. *Dalton Trans.* **2000**, 4277.

10.1021/ic060604p CCC: $33.50
Published on Web 07/12/2006

and Mo−Mo single bonds, respectively.[4] When the separation between the two dimetal units is large, the loss of δ bonding to give two new single bonds does not occur, and a molecule of type **II** is obtained. An example of this type occurs when X = I.[5] Many other compounds have two Mo_2^{6+} units separated by about 3.34 Å.[6] In most of such compounds, the dimolybdenum units are coordinated by monodentate ligands. Compounds of type **III** differ from those of types **I** and **II** in that they have two Mo_2^{4+} units supported by two three-atom bridging ligands, typically *N*,*N*′-di-*p*-anisylformamidinate (DAniF) in cis positions. These compounds, described by the general formula $[Mo_2(cis\text{-DAniF})_2]_2(\mu\text{-}X_4)$, have been reported for X = Cl and I.[7] Their structural characterization revealed that such molecules, even the chloride, retain their quadruple bonds with Mo−Mo distances of 2.12 Å and the nonbonded separations between the two Mo_2 units range from 3.6 to 3.9 Å, depending on the atomic radius of the bridging atom. For compounds of this type, cycloaddition does not occur, even though the core is similar and the bridging ligands are the same as those in group **I**, e.g., Cl^-.

In recent work with compounds with two dimolybdenum units linked by a variety of polydentate ligands (L), generally formulated as $[Mo_2]L[Mo_2]$ ($[Mo_2] = [Mo_2(DAniF)_3]^+$), it has been established that efficient metal (δ)−ligand (π^*) orbital interaction is critical to promote strong electronic communication through the linker L.[8] It has been noted that the two Mo_2 units in the halide-bridged compounds of type **III** are strongly coupled, although there is no bond between them.[9] For example, $[Mo_2(cis\text{-DAniF})_2]_2(\mu\text{-}Cl_4)$ has a large $\Delta E_{1/2}$ value of 540 mV, which corresponds to a comproportionation constant of 1.3×10^9. Because of the large comproportionation constant, oxidation of the neutral precursor gives a mixed-valence complex with the unpaired electron delocalized over all four Mo atoms.[9] It should be noted that the metal-to-ligand back-bonding mechanism proposed for $[Mo_2]L[Mo_2]$ compounds[8] may not applicable to the halide system. Because of the very short metal-to-metal separation, direct head-to-head interaction between the two δ orbitals is the more likely cause of the strong coupling. This hypothesis led us to the two general objectives for the present work: (1) to extend the study on electronic interaction with this unusual coupling system and (2) to explore approaches other than [2 + 2] cycloaddition to make a transition from nonbonding to bonding interaction in rectangular Mo_4 clusters.

Here we report a series of compounds $\{[Mo_2(cis\text{-DAniF})_2]_2(\mu\text{-}OCH_3)_4\}^{n+}$, $n = 0$ (**1**), 1 (**2**), and 2 (**3**), as well as an ethoxide analogue of **1** (**4**). All of these compounds have been characterized structurally and by various spectroscopic techniques and by DFT calculations. There is a decrease of the dimetal separation as **1** is oxidized to **2** and then to **3**, which suggests bond formation between dimetal centers that reduces the bond order between the metal atoms in the species that initially had a quadruple bond.

Experimental Section

Materials and Methods. All reactions and manipulations were performed under a nitrogen atmosphere, using either a drybox or standard Schlenk line techniques. Dichloromethane and hexanes were purified under argon using a Glass Contour solvent purification system. Methanol and ethanol were distilled over the corresponding sodium alkoxide under nitrogen. The starting materials and $[Mo_2(cis\text{-DAniF})_2(NCCH_3)_4](BF_4)_2$ were prepared following reported procedures;[10] other commercially available chemicals were used as received.

Physical Measurements. Elemental analyses were performed by Robertson Microlit Laboratories, Madison, NJ. Electronic spectra were measured on a Shimadzu UV-2501PC spectrometer in CH_2Cl_2 solution. ^{1}H NMR spectra were recorded on a Inova-300 NMR spectrometer with chemical shifts (ppm) referenced to residual $CHCl_3$ in $CDCl_3$. Cyclic voltammograms and differential pulse voltammograms were collected on a CH Instruments electrochemical analyzer with Pt working and auxiliary electrodes, Ag/AgCl reference electrode, scan rate (for CV) of 100 mV/s, and 0.10 M Bu_4NPF_6 (in CH_2Cl_2) as electrolyte. The near-IR (NIR) spectrum was measured on a Bruker TEASOR 27 spectrometer. EPR spectra were recorded using a Bruker ESP300 spectrometer.

Preparation of $[Mo_2(cis\text{-DAniF})_2]_2(\mu\text{-}OCH_3)_4$, 1. To a solution of $[Mo_2(cis\text{-DAniF})_2(NCCH_3)_4](BF_4)_2$ (416 mg, 0.400 mmol) in 20 mL of methanol was added slowly, and with stirring, 2.0 mL of a 0.50 M solution of $NaOCH_3$ in methanol. A brown precipitate formed immediately. This reaction mixture was stirred at ambient temperature for 1 h. After the supernatant solution was decanted, the remaining solid was washed with methanol (2×15 mL) and briefly dried under vacuum. The dry solid was dissolved in 15 mL of dichloromethane. After the mixture was passed through a Celite-packed frit, the filtrate was layered with methanol. Red-brown needle crystals formed in 7 days. Yield: 180 mg (59%). ^{1}H NMR (ppm in $CDCl_3$) at −50 °C: 8.82 (s, 4H, −NC*H*N−), 6.62 (m, 32H, aromatic C-*H*), 4.26 (s, 12H, −OCH_3), 3.73 (s, 24H, −CH_3 in DAniF). UV−vis, λ_{max} nm (ϵ, $M^{-1}\cdot mol^{-1}$): 500 (1.1×10^3), 420 (6.3×10^2). Anal. Calcd for $C_{64.75}H_{73.5}Mo_4N_8O_{12}Cl_{1.5}$ (**1**·0.75CH_2Cl_2): C, 48.75; H, 4.62; N, 7.05. Found: C, 48.88; H, 4.36; N, 7.14.

Preparation of $\{[Mo_2(cis\text{-DAniF})_2]_2(\mu\text{-}OCH_3)_4\}PF_6$, 2. Solutions of **1** (204 mg, 0.134 mmol in 10 mL of CH_2Cl_2) and ferrocenium hexafluorophosphate (44 mg, 0.134 mmol in 10 mL of CH_2Cl_2) were prepared separately and cooled to −78 °C. The solution of $[FeCp_2]PF_6$ was transferred to the solution of $[Mo_2(cis\text{-DAniF})_2]_2(\mu\text{-}OCH_3)_4$ using a cannula. The resulting dark brown mixture was stirred at low temperature for 30 min, and then 40 mL of precooled hexanes were added to precipitate a dark brown solid. After the yellow supernatant solution was decanted, the solid

(3) Beers, W. W. McCarley, R, E.; Martin, D. S.; Miskowski, V. M.; Gray, H. B.; Hopkins, M. D. *Coord. Chem. Rev.* **1999**, *187*, 103.
(4) McGinnis, R. N.; Ryan, T. R.; McCarley, R. E. *J. Am. Chem. Soc.* **1978**, *100*, 7900.
(5) Ryan, T. R.; McCarley R. E. *Inorg. Chem.* **1982**, *21*, 2070.
(6) Chisholm, M. H.; Hammond, C. E.; Hampden-Smith, M.; Huffman, J. C.; Van Der Sluys, W. G. *Angew, Chem., Int. Ed. Engl.* **1987**, *26*, 904.
(7) Cotton, F. A.; Daniels, L. M.; Guimet, I.; Henning, R. W.; Jordan, G. T.; Lin, C.; Murillo, C. A.; Schultz, A. J. *J. Am. Chem. Soc.* **1998,** *120*, 12531.
(8) Cotton, F. A.; Murillo, C. A.; Villagrán, D.; Yu, R. *J. Am. Chem. Soc.* **2006**, *128*, 3281.
(9) (a) Cotton, F. A.; Liu, C. Y.; Murillo, C. A.; Wang, X. *Chem. Commun.* **2003**, 2190. (b) Cotton, F. A.; Liu, C. Y.; Murillo, C. A.; Zhao, Q. Unpublished results.
(10) Chisholm, M. H.; Cotton, F. A.; Daniels, L. M.; Folting, K.; Huffman, J. C.; Iyer, S. S.; Lin, C.; Macintosh, A. M.; Murillo, C. A. *J. Chem. Soc., Dalton Trans.* **1999**, 1387.

Table 1. X-ray Crystallographic Data

compound	**1**·3CH_2Cl_2	**2**·2CH_2Cl_2	**3**·2CH_2Cl_2	**4**·2CH_2Cl_2
empirical formula	$C_{67}H_{78}Cl_6Mo_4N_8O_{12}$	$C_{66}H_{76}Cl_4PF_6Mo_4N_8O_{12}$	$C_{66}H_{76}Cl_4B_2F_8Mo_4N_8O_{12}$	$C_{70}H_{84}Cl_4Mo_4N_8O_{12}$
fw	1783.83	1843.33	1872.53	1755.01
space group	$P\bar{1}$ (No. 2)	$P\bar{1}$ (No. 2)	$P\bar{1}$ (No. 2)	$P\bar{1}$ (No. 2)
a, Å	10.3113(8)	10.067(2)	9.962(1)	10.4659(1)
b, Å	15.031(1)	12.042(3)	18.083(3)	14.7445(2)
c, Å	24.154(2)	15.385(3)	21.830(4)	14.9192(2)
α, deg	86.840(2)	89.052(4)	99.415(3)	104.812(2)
β, deg	86.569(1)	78.797(4)	92.164(3)	106.064(2)
γ, deg	89.542(2)	82.177(4)	103.810(4)	108.693(2)
V, Å^3	3731.2(5)	1812.5(7)	3755.5(1)	1939.9(4)
Z	2	1	2	1
T, K	213	213	213	213
λ, Å	0.71073	0.71073	0.71073	0.71073
d_{calcd}, g/cm^3	1.588	1.689	1.656	1.502
μ, mm^{-1}	0.934	0.926	0.878	0.831
R1[a] (wR2[b])	0.0594(0.1430)	0.0395(0.0834)	0.0899(0.1645)	0.0426(0.1120)

[a] $R1 = \sum||F_o| - |F_c||/\sum|F_o|$. [b] $wR2 = [\sum[w(F_o^2 - F_c^2)^2]/\sum[w(F_o^2)^2]]^{1/2}$.

was washed with cooled hexanes (2 × 15 mL) and then dried under vacuum. The dry solid was dissolved in 15 mL of dichloromethane in a Schlenk tube, and the solution was layered with hexanes. Dark-brown needles formed in about 1 week. Yield: 182 mg (81%). UV−vis, λ_{max} nm (ϵ, M^{-1}·mol^{-1}): 490 (2.5 × 10^3). Anal. Calcd for $C_{65}H_{74}F_6Mo_4N_8O_{12}PCl_2$ (**2**·CH_2Cl_2): C, 44.38; H, 4.24; N, 6.37. Found: C, 44.18; H, 3.81; N, 6.31.

Preparation of {$[Mo_2(cis\text{-}DAniF)_2]_2(\mu\text{-}OCH_3)_4$}$(BF_4)_2$, 3. The preparation was similar to that for **2**, but 2 equiv of oxidizing reagent $[Cp_2Fe]BF_4$ were used. For a reaction starting with **1** (152 mg, 0.100 mmol), the yield of dark crystals was 96 mg (60%). ^{1}H NMR (ppm in $CDCl_3$) at −50 °C: 9.44 (s, 4H, −NC*H*N−), 6.89(d, 16H, aromatic C−*H*), 6.69 (d, 16H, aromatic C−*H*), 4.20 (s, 12H, −OCH_3), 3.73 (s, 24H, −CH_3 in DAniF). UV−vis, λ_{max} nm (ϵ, M^{-1}·mol^{-1}): 790 (6.4 × 10^2), 580 (1.3 × 10^3). Anal. Calcd for $C_{65.5}H_{75}B_2F_8Mo_4N_8O_{12}Cl_3$ (**3**·1.5CH_2Cl_2): C, 42.99; H, 4.13; N, 6.12. Found: C, 43.39; H, 3.63; N, 5.72.

Preparation of $[Mo_2(cis\text{-}DAniF)_2]_2(\mu\text{-}OC_2H_5)_4$, 4. A procedure similar to the one described for **1**, with the same reaction scale as above, was employed for the preparation of the ethoxide analogue. For this reaction, ethanol was used instead of methanol. Yield: 160 mg (51%). UV−vis, λ_{max} nm (ϵ, M^{-1}·mol^{-1}): 500 (5.9 × 10^3), 425 (1.0 × 10^2). Anal. Calcd for $C_{69}H_{82}Mo_4N_8O_{12}Cl_2$ (**4**·CH_2Cl_2): C, 49.62; H, 4.95; N, 6.71. Found: C, 49.71; H, 4.85; N, 6.94.

X-ray Structural Determinations. Single crystals suitable for X-ray analysis were mounted on the tips of cryoloops attached to a goniometer head. Data for **1**·3CH_2Cl_2, **2**·2CH_2Cl_2, **3**·2CH_2Cl_2, and **4**·2CH_2Cl_2 were collected at −60 °C on a BRUKER SMART 1000 CCD area detector system. Cell parameters were determined using the program SMART.[11] Data reduction and integration were performed with the software SAINT,[12] while the absorption corrections were applied by using the program SADABS.[13] The structures were solved by direct methods and refined using the SHELXS-97 program.[14] Non-hydrogen atoms, except for those of disordered solvent molecules, were refined with anisotropic displacement parameters. Hydrogen atoms were added in calculated positions. Crystallographic data are given in Table 1.

Computational Details. Density functional theory (DFT)[15] calculations were performed with the hybrid Becke[16] three-parameter exchange functional and the Lee−Yang−Parr[17] non-local correlation functional (B3LYP) in the Gaussian 03 program.[18] Double-ζ-quality basis sets (D95)[19] were used on C, N, and H atoms as implemented in Gaussian. For the O atoms, correlation-consistent double-ζ basis sets (CC-PVDZ)[20] were applied. A small effective core potential (ECP) representing the 1s2s2p3s3p3d core was used for the molybdenum atoms along with its corresponding double-ζ basis set (LANL2DZ).[21] Time-dependent density functional (TD-DFT) calculations[22] were used to assign the electronic spectra of these compounds. All calculations were performed on either an Origin 3800 64-processor SGI or an Origin 2000 32-processor SGI computer located at the Texas A&M supercomputing facility.

(11) *SMART for Windows NT*, Version 5.618; Bruker Advanced X-ray Solution, Inc.: Madison, WI, 2001.

(12) *SAINT, Data Reduction Software*, version 6.36A; Bruker Advanced X-ray Solution, Inc.: Madison, WI, 2001.

(13) *SADABS, Area Detector Absorption and other Correction Software*, version 2.05; Bruker Advanced X-ray Solution, Inc.: Madison, WI, 2000.

(14) Sheldrick, G. M. *SHELXTL*, version 6.12; Advanced X-ray Solutions, Inc.: Madison, WI, 2002.

(15) (a) Hohenberg, P.; Kohn, W. *Phys. Rev.* **1964**, *136*, B864. (b) Parr, R. G.; Yang, W. *Density-Functional Theory of Atoms and Molecules*; Oxford University Press: Oxford, 1989.

(16) (a) Becke, A. D. *Phys. Rev. A* **1988**, *38*, 3098. (b) Becke, A. D. *J. Chem. Phys.* **1993**, *98*, 1372. (c) Becke, A. D. *J. Chem. Phys.* **1993**, *98*, 5648.

(17) Lee, C. T.; Yang, W. T.; Parr, R. G. *Phys. Rev. B* **1998**, *37*, 785.

(18) Frisch, M. J.; Trucks, G. W.; Schlegel, H. B.; Scuseria, G. E.; Robb, M. A.; Cheeseman, J. R.; Montgomery, J. A., Jr.; Vreven, T.; Kudin, K. N.; Burant, J. C.; Millam, J. M.; Iyengar, S. S.; Tomasi, J.; Barone, V.; Mennucci, B.; Cossi, M.; Scalmani, G.; Rega, N.; Petersson, G. A.; Nakatsuji, H.; Hada, M.; Ehara, M.; Toyota, K.; Fukuda, R.; Hasegawa, J.; Ishida, M.; Nakajima, T.; Honda, Y.; Kitao, O.; Nakai, H.; Klene, M.; Li, X.; Knox, J. E.; Hratchian, H. P.; Cross, J. B.; Bakken, V.; Adamo, C.; Jaramillo, J.; Gomperts, R.; Stratmann, R. E.; Yazyev, O.; Austin, A. J.; Cammi, R.; Pomelli, C.; Ochterski, J. W.; Ayala, P. Y.; Morokuma, K.; Voth, G. A.; Salvador, P.; Dannenberg, J. J.; Zakrzewski, V. G.; Dapprich, S.; Daniels, A. D.; Strain, M. C.; Farkas, O.; Malick, D. K.; Rabuck, A. D.; Raghavachari, K.; Foresman, J. B.; Ortiz, J. V.; Cui, Q.; Baboul, A. G.; Clifford, S.; Cioslowski, J.; Stefanov, B. B.; Liu, G.; Liashenko, A.; Piskorz, P.; Komaromi, I.; Martin, R. L.; Fox, D. J.; Keith, T.; Al-Laham, M. A.; Peng, C. Y.; Nanayakkara, A.; Challacombe, M.; Gill, P. M. W.; Johnson, B.; Chen, W.; Wong, M. W.; Gonzalez, C.; Pople, J. A. *Gaussian 03*, revision C.02; Gaussian, Inc.: Wallingford, CT, 2004.

(19) (a) Dunning, T. H.; Hay, P. J. In *Modern Theoretical Chemistry. 3. Methods of Electronic Structure Theory*; Schaefer, H. F., III, Ed.; Plenum Press: New York, 1977; pp 1−28. (b) Woon, D. E.; Dunning, T. H. *J. Chem. Phys.* **1993**, *98*, 1358.

(20) (a) Dunning, T. H. *J. Chem. Phys.* **1989**, *90*, 1007. (b) Woon, D. E.; Dunning, T. H. *J. Chem. Phys.* **1993**, *98*, 1358. (c) Wilson, A. K.; Woon, D. E.; Peterson, K. A.; Dunning, T. H. *J. Chem. Phys.* **1999**, *110*, 7667.

(21) (a) Wadt, W. R.; Hay, P. J. *J. Chem. Phys.* **1985**, *82*, 284. (b) Hay, P. J.; Wadt, W. R. *J. Chem. Phys.* **1985**, *82*, 299.

(22) Casida, M. E.; Jamorski, C.; Casida, K. C.; Salahub, D. R. *J. Chem. Phys.* **1998**, *108*, 4439.

Scheme 3

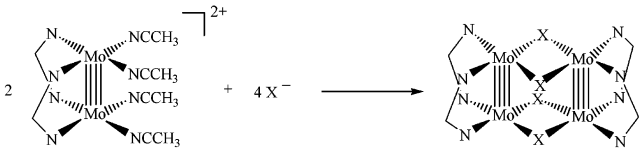

Results and Discussion

Syntheses. Compounds **1** and **4** have been prepared by direct assembly of the building block precursor $[Mo_2(cis\text{-}DAniF)_2(CH_3CN)_4](BF_4)_2$ with the corresponding bridging ligands, as described by eq 1.

$$2[Mo_2(cis\text{-}DAniF)_2(NCCH_3)_4](BF_4)_2 + 4NaOCH_3 \xrightarrow{ROH} [Mo_2(cis\text{-}DAniF)_2]_2(\mu\text{-}OR_4) + 4NaBF_4 + 8NCCH_3 \quad (1)$$

$$R = CH_3 \text{ for } \mathbf{1} \text{ and } C_2H_5 \text{ for } \mathbf{4}$$

This procedure is straightforward and appears to be applicable to the preparation of analogous compounds simply by changing the bridging ligand. For example, the halide bridged compounds $[Mo_2(cis\text{-}DAniF)_2]_2(\mu\text{-}X_4)$ (X = Cl and I) were first prepared by a complicated and time-consuming procedure.[7] Using the designed building block $[Mo_2(cis\text{-}DAniF)_2(NCCH_3)_4](BF_4)_2$, the neutral compounds of type **III** with varying bridging ligands can be prepared by the direct assembly reaction described in Scheme 3.

For the preparation of **1** and **4**, the use of alcohol as solvent is very important since it provides an additional driving force for the reaction because of the low solubility of the neutral products in such a polar solvent. In the case of **4**, ethanol is the source of the bridging ligand ethoxide. The use of alcohol consisting of the same R group as the bridging ligands benefits the formation of the product and delays hydrolysis. Therefore, this preparative route provides a general method for the preparation of analogous alkoxide-bridged Mo_4 clusters by changing the alcohol used as a solvent. It is very important to maintain rigorously water-free conditions because competition of hydroxide for the bridging positions will result in partially OH^--substituted products. Pure products were obtained only by using freshly distilled alcohols to which sodium metal had been added to form the corresponding sodium alkoxides.

The oxidized compounds **2** and **3** were prepared by oxidation of the neutral compound **1** using salts containing the mild oxidant ferrocenium cation but carefully controlling the reaction stoichiometries. The CV and DPV in CH_2Cl_2 solution for compound **1** show two reversible waves with a large separation ΔE of 554 mV. For such a strongly coupled system, the mixed-valence complexes $\{[Mo_2(cis\text{-}DAniF)_2]_2(\mu\text{-}X_4)\}^+$, e.g., **2**, are expected to be thermodynamically stable. For the halide-bridged compounds, the second redox potential of about 800 mV (vs Ag/AgCl) was far beyond the oxidizing capability of Cp_2Fe^+,[9] but replacement of X by OR lowers the oxidation potentials by about 600 mV so that the doubly oxidized compound **3** can be prepared using the ferrocenium-containing reagents. This simplifies the treatment of the reaction mixture because the reduced byproduct, ferrocene, can be easily removed by washing with hexanes. Since the precursor **1** is very sensitive to air and moisture, the oxidation reactions were carried out at low temperature and handled with great care.

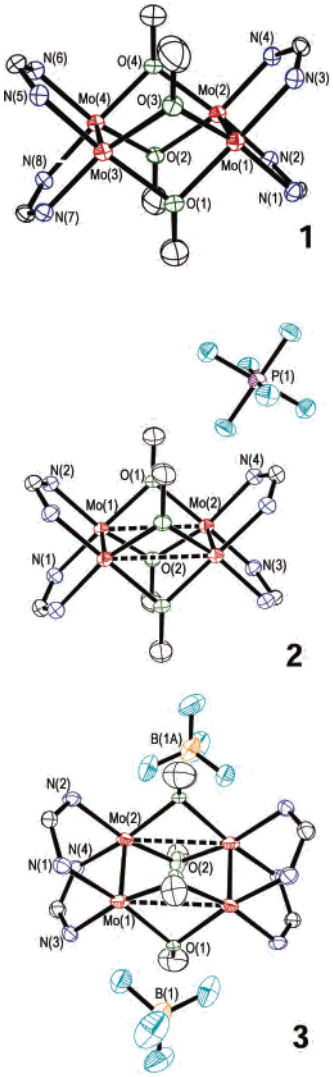

Figure 1. Cores of **1** and **2** and one of the crystallographically independent molecules in **3** with displacement ellipsoids drawn at the 40% probability level. All *p*-anisyl groups and hydrogen atoms have been omitted for clarity.

Structural Results. Compounds **1**, **2**, **3**, and **4** have been structurally characterized by single-crystal X-ray diffraction. The core structures for these molecules are shown in Figure 1 for **1**−**3** and Figure 2 for **4**. A common structural feature for these compounds is the presence of four oxygen atoms from the four alkoxide anions that bridge two parallel, DAniF-supported Mo_2 units. Such an arrangement produces a rectangular Mo_4 cluster of type **III**. This structural motif is shared by the three halide-bridged compounds $[Mo_2(cis\text{-}DAniF)_2]_2(\mu\text{-}X_4)$ (X = Cl, Br, and I).[7] These structures must not be confused with those previously reported compounds that also contain rectangular molybdenum quartets but which must be called metallacyclobutadiynes (**I**).[2,3]

The structures of the two neutral molecules **1** and **4** are very similar and have almost identical Mo−Mo, 2.132(1) Å, and other bond distances, despite the differences in the OR groups. These distances are long when compared to those

Table 2. Selected Bond Distances (Å) and Angles (deg) for Some $[Mo_2]_2(\mu\text{-}X)_4$ Compounds

	compound	charge	Mo−Mo	$Mo_2\cdots Mo_2$	Mo−X	Mo−N	Mo−X−Mo	ref
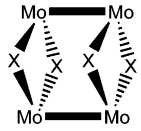	**1** (X = OMe)	0	2.1315(7)	3.245	2.142[4]	2.121[5]	98.55[16]	this work
	2 (X = OMe)	+1	2.1493(6)	3.100	2.105[1]	2.104[2]	94.81[7]	this work
	3 (X = OMe)	+2	2.1779(7)[a]	2.945	2.073[5]	2.106[5]	90.40[16]	this work
	4 (X = OEt)	0	2.1317(4)	3.241	2.136[2]	2.120[4]	98.67[9]	this work
	X = Cl	0	2.1191(4)	3.601	2.516[2]	2.095[5]	91.42[5]	7
	X = Cl	+1	2.1453(3)	3.374	2.490[6]	2.083[3]	85.28[1]	9
	X = Br	0	2.1181(6)	3.697	2.649[2]	2.093[5]	88.50[2]	9
	X = Br	+1	2.1406(9)	3.488	2.622[2]	2.091[4]	83.38[2]	9
	X = I	0	2.117(1)	3.915	2.845[2]	2.100[6]	87.02[2]	7
	X = I	+1	2.144(1)	3.632	2.812[2]	2.104[9]	80.50[4]	9

[a] See ref 28.

in other compounds containing Mo_2^{4+} units. In paddlewheel compounds, e.g., $Mo_2(O_2CCH_3)_4$ and $Mo_2(DAniF)_4$, the Mo−Mo distances are usually in the range of 2.08−2.10 Å.[23] The halide-bridged dimolybdenum diads $[Mo_2(cis\text{-}DAniF)_2]_2(\mu\text{-}X_4)$ (X = Cl, Br, and I), which are close analogues of these alkoxo compounds, have metal−metal bond distances of about 2.120 Å.[2,9] Two other species that have an Mo_2^{4+} unit supported by two cis bridging ligands and long Mo−Mo quadruple bonds are $[Mo_2(cis\text{-}DAniF)_2(CH_3CN_{eq})_4(CH_3CN_{ax})_2]^{2+}$ (2.143 Å)[10] and $[Mo_2(cis\text{-}O_2CCH_3)_2(CH_3CN_{eq})_4(CH_3CN_{ax})_2]^{2+}$ (2.134 Å).[24] For the latter, axial ligands are probably responsible for the long Mo−Mo bond distances.

A striking structural feature of **1** and **4** is the short nonbonding separation between the midpoints of the quadruply bonded units, ca. 3.24 Å, which is the shortest observed among compounds having two linked Mo_2^{4+} units. This separation is even shorter than that in the hydride-linked compound $[Mo_2(DAniF)_3]_2(\mu\text{-}H)_2$ (3.54 Å), in which a bonding interaction between the dimetal units has been suggested by DFT calculations.[25] As shown in Table 2, in the halide-bridged analogues, the two Mo_2^{4+} units are separated by 3.60−3.92 Å. Structural differences between the alkoxide- and halide-bridged families are also noted in the Mo−X−Mo angles. For **1** and **4**, all Mo−O−Mo angles are obtuse (ca. 98.5−98.6°); in contrast, the Mo−X−Mo angles (X = Cl, Br, and I) are close to a right angle (range from 87.0° to 91.4°).[9] For any given M−X bond distance, the geometric consequence of enlarging the bridging angles should be an increase in the separation between the bridged dimetal units, but the Mo−O bonds are much shorter than the Mo−X bonds.

The ^{1}H NMR spectrum of **1** at −50 °C in $CDCl_3$ shows that the molecular structure of **1** is retained in solution. A "doublet of doublets" at 6.57−6.66 ppm is attributed to the aromatic protons from the DAniF ligands, and the singlet at 8.82 ppm corresponds to the chemically equivalent methine protons. All bridging methoxy groups are equivalent, as are the methoxy groups from the anisyl groups. These resonances are consistent with the D_{2h} symmetry of the molecule in solution. At room temperature, the peak for methine protons broadens and essentially disappears and the signals for the aromatic DAniF protons appear as a broad band at 6.6 ppm. This is consistent with a fluxional process in solution.[26] Similarly, for compound **4**, there are sharp signals in the low-temperature spectrum that become broad at ambient temperature but the spectrum is complex in the alkyl region. In **4**, the four ethyl groups are embedded between two $[Mo_2(cis\text{-}DAniF)_2]^{2+}$ units and rotations about the O−C bonds are sterically blocked. There are steric repulsions between methyl groups of the two ethoxide groups on the same side of the rectangular plane defined by the four Mo atoms which generate four possible conformational isomers, as shown in Scheme 4. Indeed some of the fluxional behavior suggested by the ^{1}H NMR spectrum in $CDCl_3$ is consistent with the existence of conformational isomers.

Scheme 4

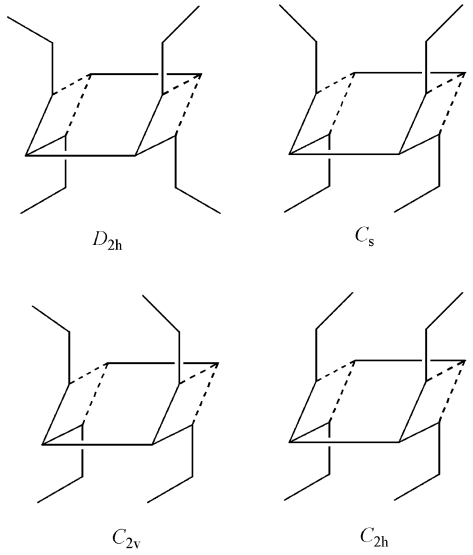

Removal of one electron from **1** gives the complex cation in **2** shown in Figure 1. Upon oxidation, the Mo−Mo bond distances are lengthened from 2.1315(7) Å in the precursor to 2.1493(3) Å (Table 2), which is consistent with an electron being removed from a bonding orbital delocalized over the dimetal units and a decrease of 0.25 in each bond order. The

(23) Cotton, F. A.; Daniels, L. M.; Hillard, E. A.; Murillo, C. A. *Inorg. Chem.* **2002**, *41*, 2466.

(24) (a) Cotton, F. A.; Reid, A. H.; Schwotzer, W. *Inorg. Chem.* **1985**, *24*, 3965. (b) Pimblett, G.; Garner, C. D. *J. Chem. Soc., Dalton Trans* **1986**, 1257.

(25) Cotton, F, A.; Donahue, J. P.; Huang, P. Murillo, C. A.; Villagrán, D. *Z. Anorg. Allg. Chem.* **2005**, *631*, 2606.

(26) Similar fluxional behavior has been observed in other systems containing linked $Mo_2(DAniF)_3$ units in close proximity. See for example: (a) Cotton, F. A.; Liu, C. Y.; Murillo, C. A.; Villagrán, D.; Wang X. *J. Am. Chem. Soc.* **2004**, *126*, 14822. (b) Cotton, F. A.; Liu, C. Y.; Murillo, C. A.; Villagrán, D.; Wang X. *J. Am. Chem. Soc.* **2003**, *125*, 13564.

increase of 0.018 Å in the Mo−Mo bond distance in going from **1** to **2** is similar to those observed in other delocalized situations but considerably less than that found in localized mixed-valence complexes $[Mo_2]^{1+}L[Mo_2]^0$.[26a,27] Accompanying the lengthening of the metal−metal bond, the $Mo_2\cdots Mo_2$ distance is reduced from 3.245 to 3.100 Å and the average bridging angles Mo−O−Mo (ca. 94.81°) become slightly smaller than those in **1** (ca. 98.55°). Similar changes have been observed in $[Mo_2(cis\text{-DAniF})_2]_2(\mu\text{-}X_4)$ (X = Cl, Br, and I) compounds as one electron is removed from the neutral complexes.[9] The metal−ligand bond distances are shortened, for example, from 2.142[4] to 2.105[1] Å for $Mo-O_{alkoxide}$ and from 2.121[5] to 2.104[2] Å for $Mo-N_{DAniF}$ because of the increase in oxidation number of the dimetal units.

The dication **3** is unique in that it is the first $Mo_4(\mu\text{-}X)_4$ cluster that has two Mo_2^{5+} units. There are two crystallographically independent molecules in the unit cell. In one of them, a BF_4 anion is at a distance of 2.547 Å from an Mo atom, while in the other species the cation is devoid of close interactions with the anions. However, the Mo−Mo and other bond distances are similar.[28] As shown in Table 2, the Mo−Mo bond distances further increase upon removal of the second electron. The lengthening of the Mo−Mo bond distances, 0.029 Å from 2.1493(6) Å in **2** to 2.1779(7) Å in **3**, is significantly larger than that from **1** to **2** (0.018 Å). As an additional one-electron oxidation occurs, the two $[Mo_2]$ units get even closer as the $Mo_2\cdots Mo_2$ separation decreases from 3.100 Å in **2** to 2.945 Å; the Mo−O−Mo angles are also reduced to 90.40° from 94.81°. Again, these changes are greater than those observed as one electron is removed from **1**. The second oxidation appears to have a direct and significant impact on the electronic configuration of the cluster. It is particularly important to note that shortening of the $Mo_2\cdots Mo_2$ separations occurred even though there are two positively charged $[Mo_2]$ units separated by a very short distance (2.945 Å). Such shortening cannot be attributed solely to small geometric changes arising from a slight decrease of the Mo−O distances (0.03 Å) from **2** to **3** (Table 2). In contrast, an increase in electrostatic repulsion between two linked Mo_2^{5+} units is known to lead to an increase in the dimetal separation in an electron-localized complex system.[29]

It also should be noted that many rectangular Mo_4 clusters characterized as metallocyclobutadiynes have short distances between two dimolybdenum units (about 2.9 Å), which have been associated with metal−metal single bonds along the long edges of the rectangle.[2] For **3**, the metal−metal separation, 2.945 Å, is very close to that for the long edges in such metallacyclobutadiynes. The Mo−Mo bond lengths of 2.1779 Å (i.e., the short edges of **3**) are exceptionally long and much longer than those in the compounds with an

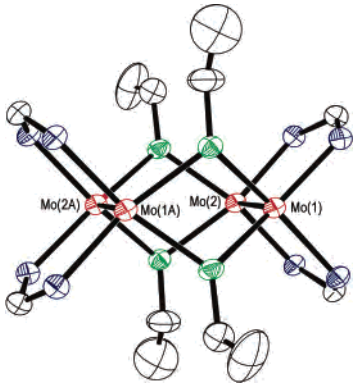

Figure 2. Core structure of **4** with displacement ellipsoids drawn at the 40% probability level. All *p*-anisyl groups and hydrogen atoms have been omitted for clarity.

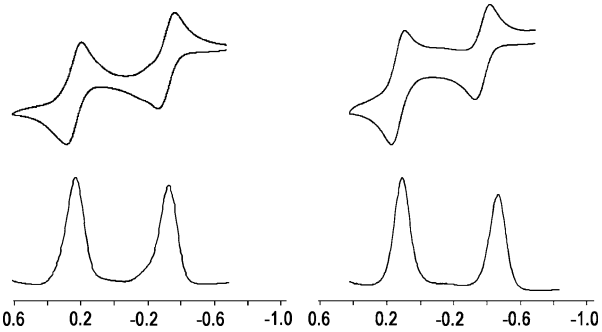

Figure 3. Cyclic voltammogram (with potentials vs Ag/AgCl) and differential pulse voltammogram (DPV) for **1** (left) and **4** (right) in CH_2Cl_2 solution.

Mo_2^{5+} core.[30] The remarkable variations in structural parameters from **1** to **3** are consistent with a bonding interaction between the two Mo_2 units being formed as the bond order of each Mo_2 unit decreases. A better understanding of the electronic configuration of **3** comes from theoretical work and will be described below.

The ^1H NMR spectrum of **3** at −50 °C in CD_3Cl closely resembles that of the neutral precursor **1**. The spectrum shows two "doublets" centered at 6.69 and 6.89 ppm which are attributed to the aromatic protons in the DAniF ligands and a singlet at 9.44 ppm for the chemically equivalent methine protons. The signals for methyl groups from the methoxy linker and those from the DAniF ligands are at 4.20 and 3.73 ppm, respectively. As in **1**, the signals for the methine and linker protons coalesce at room temperature because of a dynamic process that takes place in solution. The sharp signals in the low-temperature spectra, as well as the position of the resonances, suggest that **3** has a diamagnetic ground state.

Electrochemistry and Electronic Communication. Because of the short separation between the two bridged dimolybdenum units, a strong metal-to-metal electronic coupling interaction would be anticipated, and for **1** and **4**, electrochemical measurements (Figure 3) show two successive one-electron oxidations separated by large $\Delta E_{1/2}$ values of 554 and 587 mV, respectively. These electrochemical data

(27) Cotton, F. A.; Li, Z.; Liu, C. Y.; Murillo, C. A.; Villagrán, D. *Inorg. Chem.* **2006**, *45*, 767.
(28) The Mo−Mo distance in the unit devoid of axial interactions is 2.1704(7) Å, and that in the unit with the axial BF_4 anion is 2.1779(7) Å.
(29) Cotton, F. A.; Dalal, N. S.; Liu, C. Y.; Murillo, C. A.; North, J. M.; Wang, X. *J. Am. Chem. Soc.* **2003**, *125*, 12945.
(30) Cotton, F. A.; Daniels, L. M.; Hillard, E. A.; Murillo, C. A. *Inorg. Chem.* **2002**, *41*, 2466.

Table 3. Electrochemical Data for $[Mo_2(DAniF)_2]_2(\mu\text{-}X_4)$ Compounds

X	$Mo_2\cdots Mo_2$ (Å)	$E_{1/2}(1)$ (mV)	$E_{1/2}(2)$ (mV)	$\Delta E_{1/2}$ (mV)	K_C	ref
OMe	3.245	−338	216	554	2.3×10^9	this work
OEt	3.241	−418	169	587	8.4×10^9	this work
Cl	3.601	260	800	540	1.3×10^9	9
Br	3.697	314	813	499	2.7×10^8	9
I	3.915	350	790	440	2.7×10^7	9

along with those for $[Mo_2(cis\text{-}DAniF)_2]_2(\mu\text{-}X)_4$ compounds, are listed in Table 3, together with the comproportionation constants derived from the equation $K_C = e^{\Delta E_{1/2}/25.69}$.[31] Table 3 shows that the alkoxide-bridged compounds exhibit significantly more negative potentials than the halide-bridged analogues. The highly basic $^-$OR groups are responsible for such a shift in electrode potentials. A similar effect has been observed when comparing $[Mo_2]O_2EO_2[Mo_2]$ compounds (E = S, Mo, and W) with their structural analogues $[Mo_2](OCH_3)_2M(OCH_3)_2[Mo_2]$ (M = Zn and Co).[9,32] The exceptionally large values of $\Delta E_{1/2}$ and K_C suggest that the mixed-valence species **2** is thermodynamically stable.

For many cases in which the two metal redox sites are bridged by a polydentate ligand, back-bonding from metal to ligand is considered to be the major pathway that permits communication between the two metal centers.[8] Our studies on a variety of complexes with two $[Mo_2]$ units linked by a conjugated organic ligand have revealed that strong electronic coupling interaction entails an efficient metal (δ)−ligand (π^*) orbital interaction.[8,27] Such a pathway is not available for $[Mo_2]X_4[Mo_2]$-type compounds. For **1** and **4**, the very short metal−metal separation must be an important factor in the increased coupling effect, most likely by a direct δ-to-δ orbital interaction between the two dimetal centers (vide infra).

Magnetism and NIR Spectra. The X-band EPR spectrum for **2** measured in CH_2Cl_2 at room temperature is shown in Figure 4 along with the measurement of the doubly oxidized compound **3**. For the singly oxidized species **2**, the *g* value of 1.922, which is significantly lower than that for a free radical, indicates that the unpaired electron resides in an orbital that is mainly metal-based. The prominent symmetric peak is due to molecules containing only the ^{96}Mo ($I = 0$) isotope (about 74% in abundance), whereas the small peaks flanking around the main signal are assignable to hyperfine structure from the ^{95,97}Mo ($I = 5/2$) isotopes with natural abundance of about 25%. Compound **3**, which forms upon removal of two electrons from **1**, is diamagnetic, as suggested by the sharp ^{1}H NMR signals, and is EPR silent. The diamagnetism in **3**, in which there are, formally, two Mo_2^{5+} units, each having an unpaired electron, is caused by antiferromagnetic coupling.

The NIR spectrum of **2** in CH_2Cl_2 solution measured in the region from 4000 to 10 000 cm^{-1} (Figure 5) shows two intense absorption bands centered at 5900 (ν_1) and 7900 cm^{-1} (ν_2). Such transitions are often referred to as intervalence charge-transfer transitions. However, the spectrum of **2** is qualitatively different from those for the $[Mo_2]L[Mo_2]$ systems for which only one band has been observed in the NIR spectra.[27,33] Compounds **1** and **3** do not show bands in the NIR region.

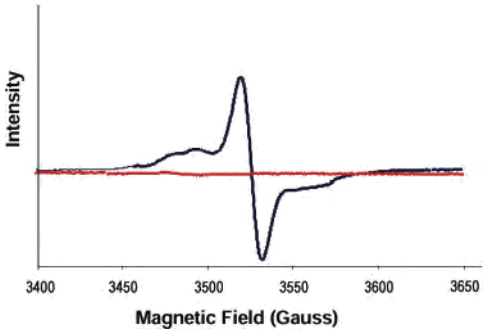

Figure 4. X-band EPR spectra of **2** (blue) and **3** (red) in CH_2Cl_2 solution at room temperature.

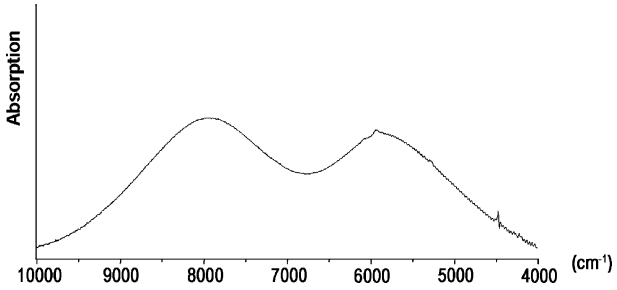

Figure 5. Near-IR spectrum of the mixed-valence species **2** in CH_2Cl_2 solution.

Table 4. Calculated Data from DFT for Models of **1**, **2**, and **3**

model	charge	total spin S	energy (au)	calculated bond lengths (Å) and angles (deg)			
				Mo−Mo	$Mo_2\cdots Mo_2$	Mo−O	Mo−O−Mo
1	0	0	−1328.5858	2.173	3.333	2.169	100.32
2	+1	1/2	−1328.4226	2.191	3.192	2.142	96.26
3	+2	0	−1328.1275	2.210	3.019	2.112	91.10
		1	−1328.1241	2.206	3.313	2.145	101.02

DFT Calculations and Electronic Structure. A series of DFT calculations were performed on the models $[(HNC(H)NH)_2Mo_2]_2(\mu\text{-}OCH_3)_4^{n+}$ ($n = 0, 1, 2$) in which the aryl groups of the formamidinate ligands were replaced by hydrogen atoms. This simplified structural model has been used successfully in similar systems.[27]

The geometries from the crystal structures of compounds **1**, **2**, and **3** were used as the starting parameters for the geometry optimization of the corresponding models. Relevant geometric and energy data obtained from the calculations are shown in Table 4. In general, the calculated Mo−Mo distances are slightly longer than the experimental values (ca. 0.04 Å), which is reasonable because in the models the *p*-anisyl groups were replaced by less-basic hydrogen atoms. All changes in bond distances and angles resulting from removal of electrons are in good agreement with those from X-ray crystallography. The calculated distance between the

(31) See, for example: (a) Flanagan, J. B.; Margel, S.; Bard, A. J.; Anson, F. C. *J. Am. Chem. Soc.* **1978**, *100*, 4248. (b) Ito, T.; Hamaguchi, T.; Nagino, H.; Yamaguchi, T.; Kido, H.; Zavarine, I. S.; Richmond, T.; Washington, J.; Kubiak, C. P. *J. Am. Chem. Soc.* **1999**, *121*, 4625.

(32) Cotton, F. A.; Donahue, J. P.; Murillo, C. A. *Inorg. Chem.* **2001**, *40*, 2229.

(33) Chisholm, M. H.; Pate, B. D.; Wilson, P. J.; Zalesky, J. M. *Chem. Commun.* **2002**, 1084.

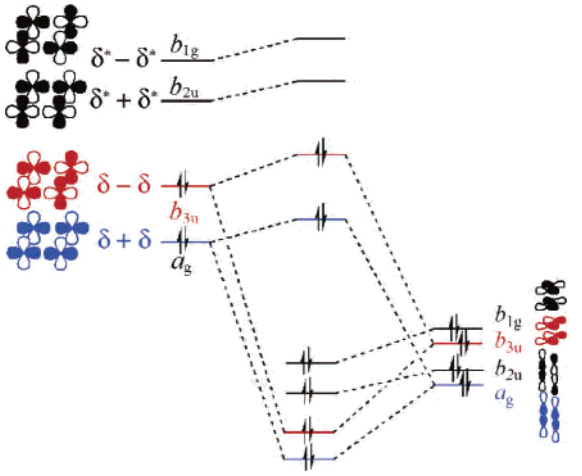

Figure 6. Frontier orbital interactions between the δ orbital combinations of the [Mo_2] units and the p orbital combinations of the oxygen atoms in the linkers.

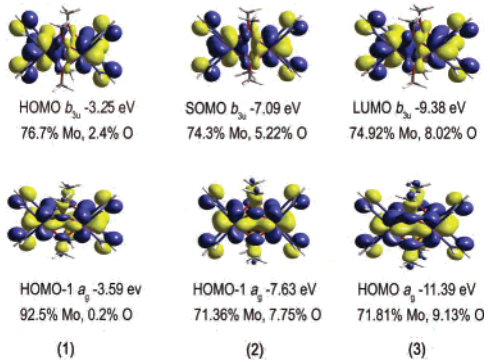

Figure 7. 0.02 surface contour diagrams for the frontier orbitals for models of **1**, **2**, and **3** calculated using DFT.

two dimetal units decreases by 0.14 Å from **1** to **2** and then by 0.17 Å from **2** to **3**; these changes are comparable with the experimental changes, which are 0.14 and 0.16 Å, respectively.

The frontier orbital interactions between the Mo_2 units and the bridging ligands are shown in Figure 6. For the model of **1**, the HOMO results from the interaction of the out-of-phase orbital of the Mo_2 units ($\delta-\delta$) with the symmetry-related combination of ligand orbitals (b_{3u}), and the HOMO-1 results from the interaction of the in-phase orbitals ($\delta + \delta$) with the matching combination of ligand orbitals (a_g). These two MOs have a large metal character: 76.7% for the HOMO and 92.5% for the HOMO-1. As shown in Figure 7, the HOMO shows antibonding character between dimetal units while the HOMO-1 has bonding character, and there is no net bonding between the two dimetal units.

The electronic structure for the model of **2** is similar to that of the precursor except for the existence of an odd electron residing in the metal-based SOMO (77.43% metal character). This is consistent with the EPR spectrum of **2** that shows a low g value of 1.92 and a χT value of 0.375. The spin density of the SOMO (Figure 8) shows that the odd electron is delocalized over the two dimolybdenum units. Because the oxidation of **1** removes one electron from the orbital which results from the metal−metal interaction between the two multiply bonded Mo_2 units and has

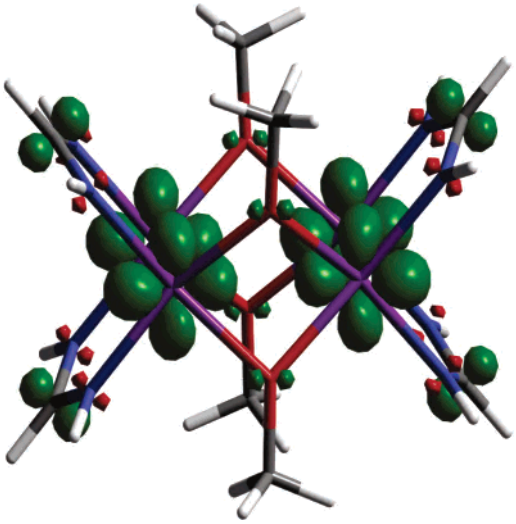

Figure 8. Illustration of the spin density for the SOMO of model **2**.

antibonding character ($\delta-\delta$), compound **2** has a bond order greater than 0 for the σ-bonding interaction between the two Mo_2 units. This represents an intermediate for the transition from a nonbonding to a bonding interaction, and explains the shortening of the $Mo_2\cdots Mo_2$ distances in going from **1** to **2**.

For the doubly oxidized compound **3**, calculations were done on models having a singlet ($S = 0$) and a triplet ($S = 1$) state. However, only the model for the singlet state is consistent with the experimental results for **3** in that it gives a contracted $Mo_2\cdots Mo_2$ distance with all other structural parameters being reasonable. The triplet state model increases the $Mo_2\cdots Mo_2$ separation, contrary to experimental observation (Table 4). The singlet state has an energy that is lower by 2.14 kcal/mol than that of the triplet state. This is again consistent with the experimental observations and further supports the diamagnetism of **3**. Furthermore, a large energy gap ($\Delta E = 2.01$ eV) is found between the LUMO and HOMO. This value is much higher than that for the singly oxidized **2**, where the model shows that the difference in energy between the SOMO and HOMO-1 is only 0.54 eV. This explains the substantial changes in structural parameters as the second electron is removed from the core of **1** compared with the changes caused by removing the first electron. Thus, on the basis of both experimental results and computational work, it is concluded that a change from a nonbonding to bonding interaction between the two Mo_2 units occurs in the course of removing two electrons from the core of **1**. In compounds of type **I**, two single bonds between two dimolybdenum units are generated by a [2 + 2] cycloaddition. For comparison with present results, this could be formally called a four-electron, four-center bond, as implied by the upper part of Scheme 5. In the case of compound **3**, a four-center, two-electron bond is formed in the cyclometallic Mo_4 cluster, as illustrated by the lower part of Scheme 5. In a very approximate way, an average bond order of 0.25 may be assigned to the bonding interaction between the two Mo atoms along the long edges of the rectangle.

Finally, TD-DFT calculations were also performed on the models of **1**, **2**, and **3** to help with the understanding of the

Scheme 5

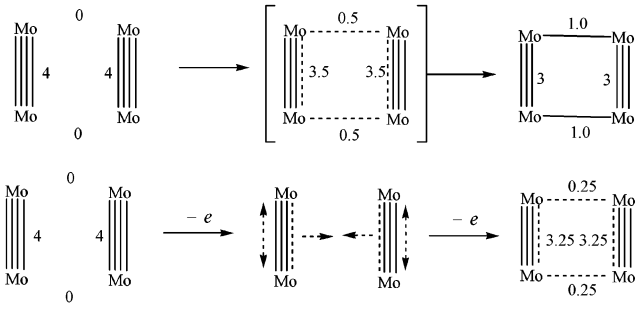

spectroscopic properties of these compounds. Two bands at 586 and 546 nm attributed to transitions from the HOMO-1 to LUMO ($\delta + \delta \rightarrow \delta^* + \delta^*$) and HOMO to LUMO+1 ($\delta - \delta \rightarrow \delta^* - \delta^*$) are calculated for the model of **1**. These calculated bands correspond to experimental absorptions at 500 and 420 nm, respectively. For the mixed-valence species **2**, two intense (*f* of ca. 0.046) absorptions resulting from the transitions of HOMO-1 → SOMO and HOMO-2 → SOMO[34] are predicted. These bands appear in the NIR spectrum of **2** (Figure 5) at 5900 and 7900 cm^{-1}. A $\delta + \delta \rightarrow \delta^* + \delta^*$ transition was calculated at 632 nm and assigned for the absorption band at 487 nm. For the doubly oxidized species **3**, HOMO → LUMO and HOMO-1 → LUMO transitions are predicted, and these bands appear in the electronic spectrum at 790 and 580 nm, respectively.

Concluding Remarks. Tetranuclear Mo_4 clusters with two quadruply bonded Mo_2^{4+} units, $[Mo_2(cis\text{-}DAniF)_2]$ linked by methoxide, **1**, and ethoxide groups, **4**, have been prepared by direct assembly from the building block $[Mo_2(cis\text{-}DAniF)_2(CH_3CN)_4]^{2+}$ with the corresponding bridging ligands. The nonbonding separation between the midpoints of the quadruply bonded units, ca. 3.24 Å, is the shortest among compounds having two linked Mo_2^{4+} units. A significant amount of direct δ-to-δ orbital interaction between the two dimetal centers occurs and accounts for the large electronic coupling between the dimetal units, as shown by the $\Delta E_{1/2}$ values of 554 and 587 mV for **1** and **4**, respectively.

When compound **1** was chemically oxidized using 1 equiv of ferrocenium to the mixed-valence species **2** by removal of one electron from a bonding orbital of the dimetal units, the Mo−Mo bond distances were lengthened from 2.1315(7) to 2.1493(3) Å, but the separation between dimetal units was shortened by about 0.14 Å. This compound shows two broad absorption bands in the NIR region at 5900 and 7900 cm^{-1}, and they are assigned to the HOMO-1 → SOMO and HOMO-2 → SOMO transitions, respectively.

The doubly oxidized compound **3** is diamagnetic, as shown by the sharp signals in the ^1H NMR spectra and the lack of an EPR signal. The Mo−Mo bond lengths, or the short edges of the Mo_4 rectangle in **3**, increase to 2.1779 Å, a distance that is exceptionally long as compared to those in compounds with a Mo_2^{5+} core.[30] The metal−metal separation, or the long edges of the rectangle, of 2.945 Å is shorter by about 0.16 Å than those in **2** and are close in length to the long edges in metallacyclobutadiynes. DFT calculations together with the experimental results lead us to conclude that a four-center, two-electron bond is formed in the cyclometallic Mo_4 cluster **3**.

In this $[Mo_2]_2(\mu\text{-}OMe)_4$ system, a transformation from a neutral compound **1** with no bonding interaction between the two Mo_2 units to a doubly oxidized compound **3** that has a bonding interaction between the two dimolybdenum units was observed; this occurs via an intermediate state having a singly oxidized mixed-valence species **2** that exhibits large electronic communication.

Acknowledgment. We thank the National Science Foundation, the Robert A. Welch Foundation, and Texas A&M University for financial support.

Supporting Information Available: X-ray crystallographic data for **1**·$3CH_2Cl_2$, **2**·$2CH_2Cl_2$, **3**·$2CH_2Cl_2$, and **4**·$2CH_2Cl_2$ in CIF format. This material is available free of charge via the Internet at http://pubs.acs.org.

IC060604P

(34) The HOMO-1 (a_g) and SOMO (b_{3u}) are the in-phase and out-of-phase combinations of δ orbitals, and the HOMO-2 (a_g) is an in-phase combination of π orbitals from the Mo_2 units.